Supporting Information

Pai et al. 10.1073/pnas.1216336110

SI Methods

Fly Strains. The fly lines used were wild-type Canton-S w^{1118} (iso1CJ); lexAop-rCD2::GFP and UAS-Dscam[1.7]::GFP (from T. Lee, Howard Hughes Medical Institute, Ashburn, VA); UAS-CD4::GFP1-10 and lexAop-CD4::GFP11 (from K. Scott, University of California, Berkeley, CA); UAS-GCaMP1.6 (from D. Reiff, Max-Planck-Institute of Neurobiology, Martinsried, Germany); E0067-Gal4 (275Y-Gal4) and c708a-Gal4 (from S. Benzer, Caltech, Pasadena, CA); UAS-dcreb2-b (from L. Davis, Baylor College of Medicine, Houston); UAS-orb2^{RNAi} (from K. Si, Stowers Institute for Medical Research, Kansas City, MO); UAS-fmr^{RNAi} (1–7) and UAS-fmr^{RNAi} (2–1) (from T. Tully); UAS-CaMKII^{hpn} (from S. Kunes, Harvard University, Cambridge, MA); UAS-HRP::CD2 (from L. Luo, Stanford University, Standford, CA). UAS-ricin^{cs} was obtained from C. J. O'Kane (University of Cambridge, Cambridge, UK), but modified in Chiang's laboratory. UAS-dsNR1, UAS-dsNR2, UAS-mKO, L0124-LexA, L5147-LexA, L5256-LexA, and L05275-LexA were generated in Chiang's laboratory. G0239-Gal4 (12639), E1132-Gal4 (112800), UAS-syt::GFP (6924 and 6926), UAS-mCD8::GFP (5137 and 5130) and alpha-lobes-absent (ala) (9463) were derived from Bloomington Stock Center. NP1528-Gal4 was obtained from the *Drosophila* Genomics Resource Center. UAS-creb2^{RNAi} (v101512), UAS-stau^{RNAi} (v106645), and UAS-pum^{RNAi} (v101399) were obtained from the Vienna *Drosophila* Resource Center. UAS-orb^{RNAi}(R1) (II, 10868R-1) and UAS-orb^{RNAi}(R5) (II, 10868R-5) were obtained from the National Institute of Genetics. All flies used for behavior assays were outcrossed with wild-type flies for five generations.

Genotypes. The following genotypes are used in Fig. 1*A*: (1) E0067-Gal4/+;UAS-mCD8::GFP/+;UAS-mCD8::GFP/+, (2) E1132-Gal4/+;UAS-mCD8::GFP/+;UAS-mCD8::GFP/+, and (3) G0239-Gal4/UAS-mCD8::GFP;UAS-mCD8::GFP/+.

The following genotypes are used in Fig. 1*B*: (1) +/+, (2) UAS-ricin^{cs}/+, (3) E0067-Gal4/+, (4) E1132-Gal4/+, (5) G0239-Gal4/+, (6) E0067-Gal4/+;;UAS-ricin^{cs}/+, (7) E1132-Gal4/+;;UAS-ricin^{cs}/+, and (8) G0239-Gal4/+;UAS-ricin^{cs}/+.

The following genotypes are used in Fig. 1*C*: (1) E0067-Gal4/+;UAS-mKO,UAS-mKO/+;UAS-Dscam::GFP/+, (2) UAS-syt::GFP/E0067-Gal4;UAS-mKO,UAS-mKO/+, (3) E0067-Gal4/+;L0124-LexA/+;lexAop-mCD4::spGFP$_{11}$,UAS-mCD4::spGFP$_{1-10}$/+, (4) E1132-Gal4/+;UAS-mKO,UAS-mKO/+;UAS-Dscam::GFP/+, (5) UAS-syt::GFP/E1132-Gal4;UAS-mKO,UAS-mKO/+, (6) E1132-Gal4/+;L0124-LexA/+;lexAop-mCD4::spGFP$_{11}$,UAS-mCD4::spGFP$_{1-10}$/+, (7) G0239-Gal4/UAS-mKO,UAS-mKO;UAS-Dscam::GFP/+, (8) UAS-syt::GFP/+;G0239-Gal4/UAS-mKO,UAS-mKO, and (9) G0239-Gal4/L0124-LexA;lexAop-mCD4::spGFP$_{11}$,UAS-mCD4::spGFP$_{1-10}$/+.

The following genotypes are used in Fig. 2*A*: (1) +/+, (2) G0239-Gal4/+, (3) UAS-shi^{ts1}/+;;UAS-shi^{ts1}/+, and (4) UAS-shi^{ts1}/+;G0239-Gal4/+;UAS-shi^{ts1}/+.

The following genotypes are used in Fig. 2*B*: (1) +/+, (2) G0239-Gal4/+, (3) UAS-shi^{ts1}/+;;UAS-shi^{ts1}/+ and (4) UAS-shi^{ts1}/+;G0239-Gal4/+;UAS-shi^{ts1}/+.

The following genotypes are used in Fig. 2*C*: G0239-Gal4/UAS-GCaMP1.6 and Fig. 2*D*: G0239-Gal4/UAS-GCaMP1.6.

The following genotypes are used in Fig. 3*A*: (1) +/+, (2) G0239-Gal4/+;UAS-Gal80^{ts}/+, (3) UAS-dcreb2-b/+, and (4) UAS-dcreb2-b /+;G0239-Gal4/+;UAS-Gal80^{ts}/+.

The following genotypes are used in Fig. 3*B*: (1) +/+, (2) G0239-Gal4/+;UAS-Gal80^{ts}/+, (3) UAS-creb2^{RNAi}/+, and (4) G0239-Gal4/UAS-creb2^{RNAi};UAS-Gal80^{ts}/+.

The following genotypes are used in Fig. 3*C*: (1) +/+, (2) G0239-Gal4/+;UAS-Gal80^{ts}/+, (3) UAS-dsNR2/+;UAS-dsNR1/+, and (4) G0239-Gal4/UAS-dsNR2;UAS-dsNR1/UAS-Gal80^{ts}.

The following genotypes are used in Fig. 3*D*: (1) +/+, (2) G0239-Gal4/+;UAS-Gal80^{ts}/+, (3) UAS-orb2^{RNAi}/+, and (4) UAS-orb2^{RNAi}/+;G0239-Gal4/+;UAS-Gal80^{ts}/+.

The following genotypes are used in Fig. 3*E*: (1) +/+, (2) G0239-Gal4/+;UAS-Gal80^{ts}/+, (3) UAS-orb^{RNAi}(R1)/+, and (4) G0239-Gal4/+;UAS-Gal80^{ts}/UAS-orb^{RNAi}(R1).

The following genotypes are used in Fig. 3*F*: (1) +/+, (2) G0239-Gal4/+;UAS-Gal80^{ts}/+, (3) UAS-orb^{RNAi}(R5)/+, and (4) G0239-Gal4/+;UAS-Gal80^{ts}/UAS-orb^{RNAi}(R5).

The following genotypes are used in Fig. 3*G*: (1) +/+, (2) G0239-Gal4/+;UAS-Gal80^{ts}/+, (3) UAS-CaMKII^{hpn}/+, and (4) G0239-Gal4/+;UAS-Gal80^{ts}/UAS-CaMKII^{hpn}.

The following genotypes are used in Fig. 3*H*: (1) +/+, (2) G0239-Gal4/+;UAS-Gal80^{ts}/+, (3) UAS-fmr^{RNAi}(1-7)/+, and (4) G0239-Gal4/+;UAS-Gal80^{ts}/UAS-fmr^{RNAi}(1–7).

The following genotypes are used in Fig. 3*I*: (1) +/+, (2) G0239-Gal4/+;UAS-Gal80^{ts}/+, (3) UAS-fmr^{RNAi}(2-1)/+, and (4) G0239-Gal4/+;UAS-Gal80^{ts}/UAS-fmr^{RNAi}(2–1).

The following genotypes are used in Fig. 3*J*: (1) +/+, (2) G0239-Gal4/+;UAS-Gal80^{ts}/+, (3) UAS-stau^{RNAi}/+, and (4) G0239-Gal4/ UAS-stau^{RNAi};UAS-Gal80^{ts}/+.

The following genotypes are used in Fig. 3*K*: (1) +/+, (2) G0239-Gal4/+;UAS-Gal80^{ts}/+, (3) UAS-pum^{RNAi}/+, and (4) G0239-Gal4/UAS-pum^{RNAi};UAS-Gal80^{ts}/+.

In Vivo GCaMP Imaging. Sample preparation was as previously described (1). Time-lapse recording of changes in GCaMP intensity before and after odor stimulations was performed on Zeiss LSM 7MP with a 40× Achroplan IR lens (0.8 NA, Zeiss). Two-photon excitation with a titanium:sapphire laser locked at 910 nm and a GaAsP detector in LSM 7MP were used for the emissions passing through a 500–550 nm band pass filter. Images were acquired with 512 × 512 pixel resolution at two frames per second for 100 frames. Odorants were delivered at 10–15 s in each 25-s trial. For naïve flies' responses to different odors, we calculated the increasing GCaMP fluorescence as $\Delta F(F_t - F_0)/F_0$. Changes in GCaMP fluorescent intensity for CS+ vs. CS− odors were calculated as $\log_{10}(\Delta F_{CS+}/\Delta F_{CS-})$.

EM Preparation. Processing of HRP-labeled tissues for electron microscopy was as previously described (1). Briefly, dissected fly brains were prefixed in 0.2% glutaraldehyde for 30 min at room temperature. Diamnobenzadine chromogenic reaction was properly held until neural processes from MB vertical lobe V3 (MB-V3) extrinsic neurons and Kenyon cells (KC) were visible. The labeled brains were postfixed with OsO_4, embedded, and sectioned. The ultrastructural images were collected with Hitachi HT7700.

Plasticity. Both antennae of adult flies collected immediately after eclosion were removed. The flies were single raised in 1.5 mL Eppendorf with 0.1 mL of medium at the bottom and kept at 25 °C for 3 wk before dissection.

Whole-Mount Immunostaining. Brain samples were prepared as described (1). The brains were incubated with the following antibody concentrations: 1:100 mouse anti-discs large (DLG);

1:10 mouse anti-FASII(1D4) (from V. Budnik, University of Massachusetts Medical School, Worcester, MA); 1:500 rabbit anti-ORB2(Ab273) (from K. Si, Stowers Institute for Medical Research); 1:50 mouse anti-ORB(4H8) (from Hybridoma Center, The Washington University School of Medicine in St. Louis, St. Louis); 1:1,000 rabbit anti-CaMKII (from L. C. Griffith, Brandeis University, Waltham, MA); 1:50 mouse anti-FMR (from F. V. Bolduc, University of Alberta, Edmonton, Alberta, Canada); 1:200 goat anti-mouse or anti-rabbit biotin (Invitrogen); and 1:500 SA 635 (Invitrogen).

Quantification of Antibody Labeling. For each targeted structure, a single optical section was taken under the same recording condition. In each sample, the mean intensity value (total intensity/total area) in MB-V3 cell body and that in ellipsoid body (EB) were measured, and the ratio (MB-V3/EB) was calculated.

1. Watts RJ, Schuldiner O, Perrino J, Larsen C, Luo L (2004) Glia engulf degenerating axons during developmental axon pruning. *Curr Biol* 14(8):678–684.

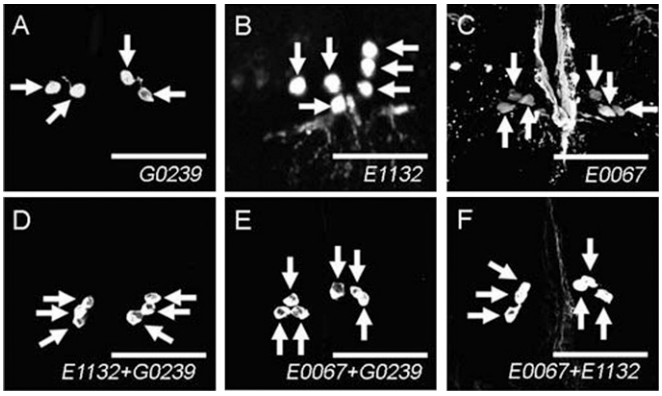

Fig. S1. *E0067-*, *E1132-*, and *G0239-Gal4* each drive reporter gene expression in MB-V3 neurons. (*A*) Four MB-V3 cells in *G0239-Gal4>UAS-mCD8::GFP* flies. (*B*) Six cells in *E1132-Gal4>UAS-mCD8::GFP* flies. (*C*) Six cells in *E0067-Gal4>UAS-mCD8::GFP* flies. (*D–F*) Only six cells were labeled in three different double combinations of these Gal4 drivers, suggesting that all three Gal4 lines contain the same MB-V3 neurons. (Scale bars, 50 μm.) Arrow, cell body near the esophagus. Genotypes: (*A*) *G0239-Gal4/UAS-mCD8::GFP*. (*B*) *E1132-Gal4/+;UAS-mCD8::GFP/+*. (*C*) *E0067-Gal4/+;UAS-mCD8::GFP*. (*D*) *E1132-Gal4/+;G0239-Gal4/UAS-mCD8::GFP*. (*E*) *E0067-Gal4/+;G0239-Gal4/UAS-mCD8::GFP*. (*F*) *E0067-Gal4/E1132-Gal4;UAS-mCD8::GFP/+*.

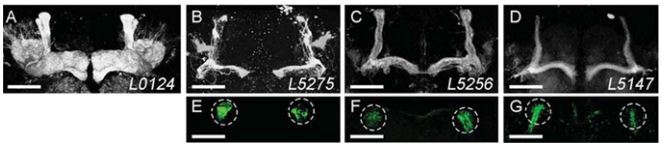

Fig. S2. Visualization of putative synaptic connections between MB-V3 and MB neurons using GFP Reconstitution Across Synaptic Partners (GRASP). (*A*) *L0124-LexA* was expressed in all MB lobes. (*B*) *L5275-LexA* was expressed in pioneer α/β neurons. (*C*) *L5256-LexA* was expressed in early α/β neurons. (*D*) *L5147-LexA* was expressed in late α/β neurons. The LexA expression pattern was labeled with *lexAop-rCD2::GFP*. (*E–G*) GRASP signals (green) showed direct contact between MB-V3 neurons and pioneer α/β neurons (*E*), early α/β neurons (*F*), or late α/β neurons (*G*) at the tips of the α/β lobes (dotted circles). (Scale bar, 50 μm.) Genotypes: (*A*) *L0124-LexA/lexAop-rCD2::GFP*. (*B*) *lexAop-rCD2::GFP/+;;L5275-LexA/+*. (*C*) *lexAop-rCD2::GFP/+;L5256-LexA/+*. (*D*) *lexAop-rCD2::GFP/+;;L5147-LexA/+*. (*E*) *G0239-Gal4/+; lexAop-mCD4::spGFP$_{11}$,UAS-mCD4::spGFP$_{1-10}$/+;L5257-LexA/+*. (*F*) *G0239-Gal4/+; lexAop-mCD4::spGFP$_{11}$,UAS-mCD4::spGFP$_{1-10}$/L5256-LexA*. (*G*) *G0239-Gal4/+; lexAop-mCD4::spGFP$_{11}$,UAS-mCD4::spGFP$_{1-10}$/+;L5147-LexA/+*.

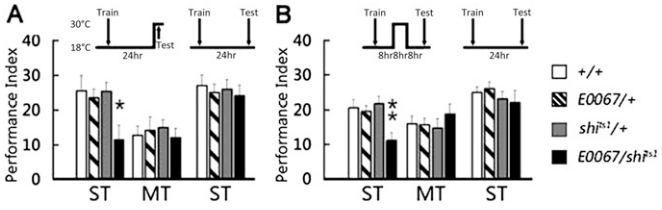

Fig. S3. The roles of neurotransmission from *E0067-Gal4* neurons in long-term memory (LTM). (*A*) Blocking neurotransmission from *E0067-Gal4* neurons during memory retrieval impaired 1-d memory after spaced training (ST) ($P = 0.035$; $n = 8$) but not after massed training (MT). Experimental flies were raised at 18 °C and shifted to 30 °C during test. Control flies kept constantly at 18 °C showed normal 1-d memory. Values are means ± SEM. (*B*) Blocking neurotransmission from *E0067-Gal4* neurons from 8 to 16 h after training impaired 1-d memory after spaced training ($P = 0.005$; $n = 12$) but not after massed training. Values are means ± SEM. Control flies kept constantly at 18 °C showed normal 1-d memory. Genotypes: (1) +/+, (2) *E0067-Gal4/+*, (3) *UAS-shi^{ts1}/+;;UAS-shi^{ts1}/+*, and (4) *E0067-Gal4/UAS-shi^{ts1};;UAS-shi^{ts1}/+*.

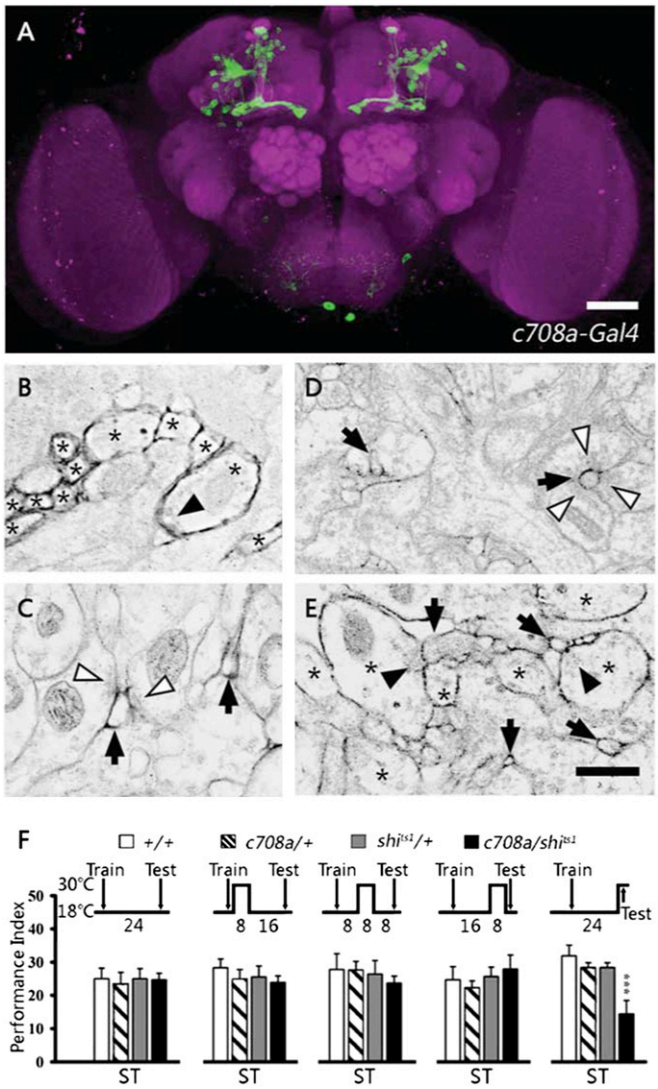

Fig. S4. Structural and functional connectivity between MB α/β axons and MB-V3 dendrites. (*A*) Expression of GFP by *c708a-Gal4* is specific to pioneer α/β MB neurons (Kenyon cells). Brain structures were immunostained with anti-DLG (magenta). (Scale bars, 50 μm.) (*B–E*) EM micrograph of HRP labeling at the tip of α lobe. In *c708a-Gal4* > *UAS-HRP::CD2* flies (*B*), cross-sections of HRP-positive axons (as indicated by the black membrane) of pioneer α/β axons (stars) were variable in size and often contained presynaptic terminals (arrowheads show clusters of neurosecretory vesicles docking to the membrane). In *G0239-Gal4* > *UAS-HRP::CD2* flies (*C*), HRP-positive dendrites of MB-V3 neurons (arrows) were always small in size and often synapsed with large HRP-negative axons containing presynaptic terminals (white arrowheads). In the flies with HRP expression in both α/β Kenyon cells and MB-V3 neurons (*D* and *E*), small HRP-positive dendrites (arrows) from MB-V3 neurons synapsed with HRP-negative axons (white arrowheads) at the tip of core α lobe, where pioneer α/β Kenyon cell axons were absent (*D*), and synapsed with HRP-positive axons (black arrowheads) at the tip of peripheral α lobe where pioneer α/β Kenyon cell axons (stars) were present (*E*). (Scale bar, 500 nm.) (*F*) Functional connectivity between pioneer α/β Kenyon cells and MB-V3 neurons. Twenty-four-hour memory after spaced training (ST) was impaired by blocking the neurotransmission from *c708a-Gal4* neurons during retrieval, but not consolidation. Genotypes: (*A*) *c708a-Gal4*/+; *UAS-mCD8::GFP*/+, (*B*) *w,UAS-HRP::CD2/c708a-Gal4*, (*C*) *w,UAS-HRP::CD2*/+;*G0239-Gal4*/+, (*D* and *E*) *w,UAS-HRP::CD2/c708a-Gal4;G0239-Gal4*/+, (*F*) (1) +/+, (2) *c708a-Gal4*/+, (3) *UAS-shi^{ts1}*/+;;*UAS-shi^{ts1}*/+, and (4) *c708a-Gal4/UAS-shi^{ts1}*;;*UAS-shi^{ts1}*/+.

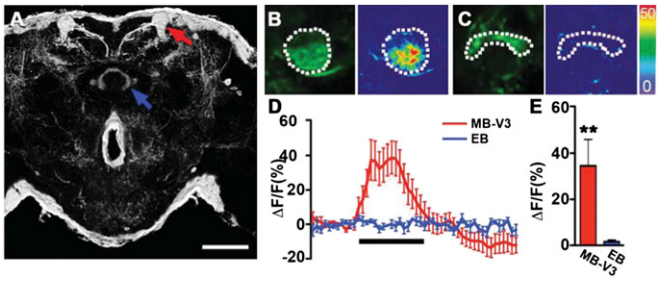

Fig. S5. GCaMP changes in the MB-V3 dendrites and ellipsoid body (EB). (*A*) An optical section through the tip of α lobe and the EB in a *E0067-Gal4* > *UAS-GCaMP1.6* fly. GCaMP intensity in the EB (blue arrow) was used as an internal control to monitor changes in the MB-V3 dendrites (red arrow). (Scale bars, 50 μm.) (*B* and *C*) Representative images of GCaMP fluorescence in the MB-V3 dendrites (*B*, dotted circle) and the EB (*C*, dotted circle), before (*Left*) and during (*Right*) 3-octanol (OCT) odor stimulation. Color coding indicates percentage of fluorescence change ranging from 0 to 50%. (*D* and *E*) The time course and peak response in the MB-V3 dendrites (red) and the EB (blue) during 25-s assay. Black bar indicates the 5-s duration of OCT stimulation. Each value represents the mean ± SEM ($n = 6$; $^{**}P < 0.01$). Genotype: *E0067-Gal4/+;UAS-GCaMP1.6/+*.

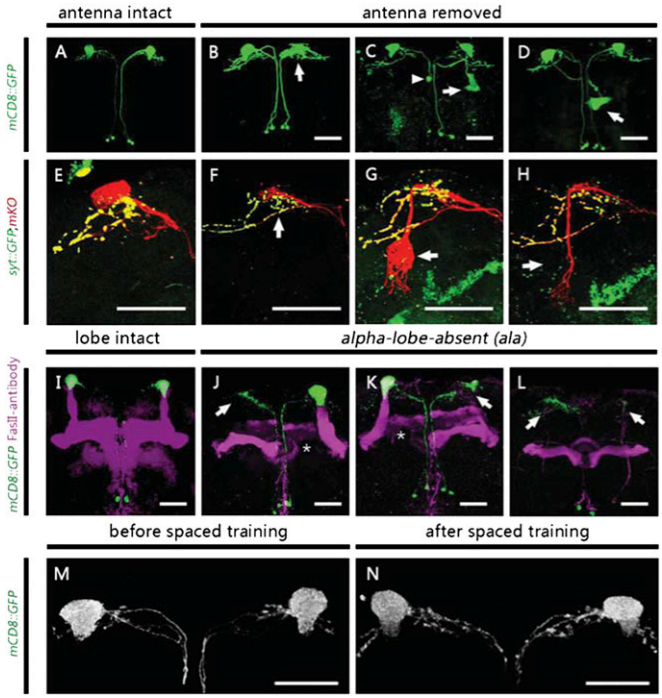

Fig. S6. Developmental plasticity of MB-V3 neuronal structure. (*A*) Morphology of MB-V3 neurons in the wild-type flies with intact antenna. (*B–D*) In flies without antennae since adult emergence, MB-V3 neurons show differing degrees of morphological deformity: unrestricted arborization (arrow in *B*), misplaced cell body (arrowhead in *C*), overshooting fibers (arrow in *C*) and additional branch (arrow in *D*). (*E–H*) Higher magnification of MB-V3 terminal fibers. Axonal terminals labeled by syt::GFP (green) remained normal. Dendritic arborizations labeled by monomeric Kusabira orange (mKO) (arrow, red) in the MB α lobe showed various degrees of structural abnormalities. (*I–L*) Developmental deformation of the MB-V3 neurons in alpha-lobe-absence (*ala*) mutant. MB-V3 neurons or MB α/β lobes were labeled by mCD8::GFP (green) or anti-FasII(1D4) immunostain (magenta), respectively. In flies with normal MB, MB-V3 neurons showed intact cluster at the tip of α lobes (*I*). In the absence of vertical lobes (arrow in *J–L*), MB-V3 neurons still projected to the same location, but dendrites show little arborization. In contrast, MB-V3 neurons developed normally in the absence of medial lobes (star in *J* and *K*). (*M* and *N*) Morphology of the MB-V3 neurons remained similar before (*M*) and after (*N*) spaced training. (Scale bar, 50 μm.) Genotypes: (*A–C*) $^{+/+}$*;G0239-Gal4/UAS-mCD8::GFP;UAS-mCD8::GFP/+*. (*D–F*) $^{+/+}$*; G0239-Gal4/UAS-mKO;UAS-syt::GFP/+*. (*G–L*) *ala/y;G0239-Gal4/UAS-mCD8::GFP;UAS-mCD8::GFP/+*. (*M* and *N*) $^{+/+}$*;G0239-Gal4/UAS-mCD8::GFP;UAS-mCD8::GFP/+*.

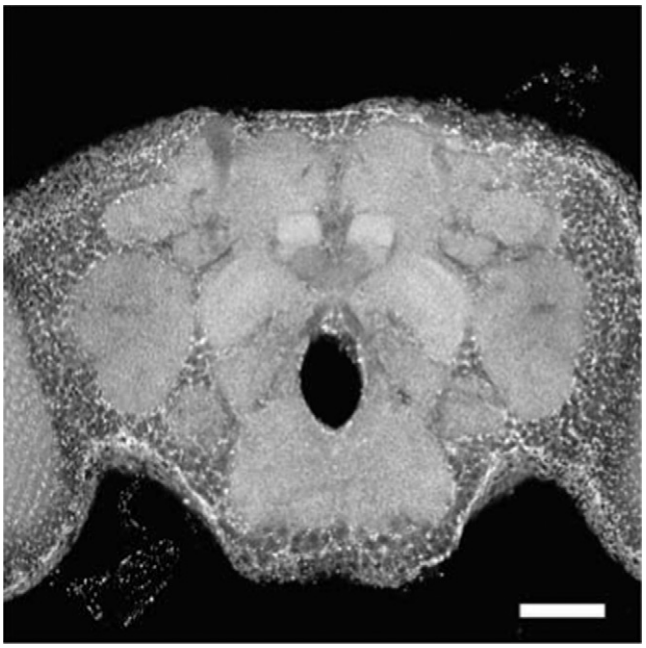

Fig. S7. Anti-ORB immunopositive signals are widely distributed in most if not all neurons in the *Drosophila* brain. (Scale bar, 50 μm.)

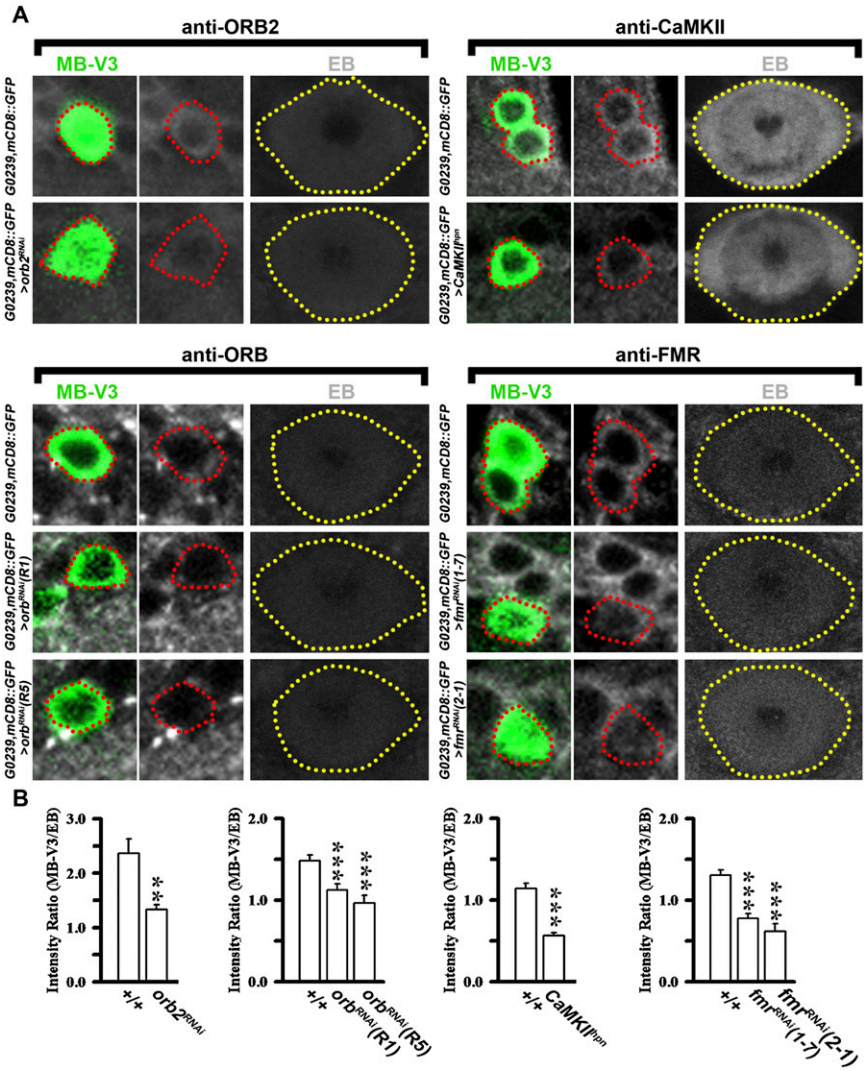

Fig. S8. RNAi and antibody specificity. (*A*) Each image of either MB-V3 cell body (red dot circle) or ellipsoid body (EB, yellow dot circle), is a single optical section taken under the same recording condition. (*B*) The ratio of immunostaining intensity between MB-V3 cell body and ellipsoid body. Values are means ± SEM ($n \geqq 8$ for each group; $P^{**} < 0.005$, $P^{***} < 0.001$). Genotypes: (1) *G0239-Gal4/+;UAS-mCD8::GFP/+*, (2) *UAS-orb2^{RNAi}/+;G0239-Gal4/+;UAS-mCD8::GFP/+*, (3) *G0239-Gal4/+;UAS-mCD8::GFP/UAS-orb^{RNAi}(R1)*, (4) *G0239-Gal4/+;UAS-mCD8::GFP/UAS-orb^{RNAi}(R5)*, (5) *G0239-Gal4/+;UAS-mCD8::GFP/UAS-CaMKII^{hpn}*, (6) *G0239-Gal4/+;UAS-mCD8::GFP/UAS-fmr^{RNAi}(1–7)*, and (7) *G0239-Gal4/+;UAS-mCD8::GFP/UAS-fmr^{RNAi}(2–1)*.

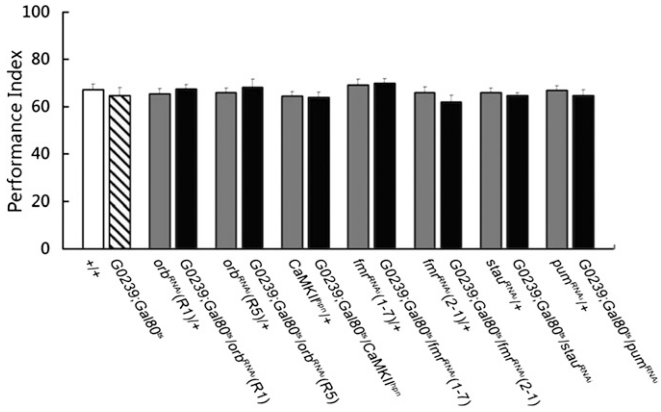

Fig. S9. Normal learning in the flies with RNAi-mediated down-regulation in MB-V3 neurons. All flies were raised at 18 °C to inhibit Gal4 with Gal80^{ts} throughout development, and shifted to 30 °C 3 d before spaced training to induce Gal4-driven RNAi activity. Values are means ± SEM ($n \geqq 8$ for each group). Genotypes: (1) +/+ and (2) *G0239-Gal4/+;UAS-Gal80^{ts}/+*, (3) *UAS-orb^{RNAi}(R1)/+* and (4) *G0239-Gal4/+;UAS-Gal80^{ts}/UAS-orb^{RNAi}(R1)*, (5) *UAS-orb^{RNAi}(R5)/+* and (6) *G0239-Gal4/+;UAS-Gal80^{ts}/UAS-orb^{RNAi}(R5)*, (7) *UAS-CaMKII^{hpn}/+* and (8) *G0239-Gal4/+;UAS-Gal80^{ts}/UAS-CaMKII^{hpn}*, (9) *UAS-fmr^{RNAi}(1-7)/+* and (10) *G0239-Gal4/+;UAS-Gal80^{ts}/UAS-fmr^{RNAi}(1–7)*, (11) *UAS-fmr^{RNAi}(2–1)/+* and (12) *G0239-Gal4/+;UAS-Gal80^{ts}/UAS-fmr^{RNAi}(2–1)*, (13) *UAS-stau^{RNAi}/+* and (14) *G0239-Gal4/ UAS-stau^{RNAi};UAS-Gal80^{ts}/+*, (15) *UAS-pum^{RNAi}/+* and (16) *G0239-Gal4/ UAS-pum^{RNAi};UAS-Gal80^{ts}/+*.

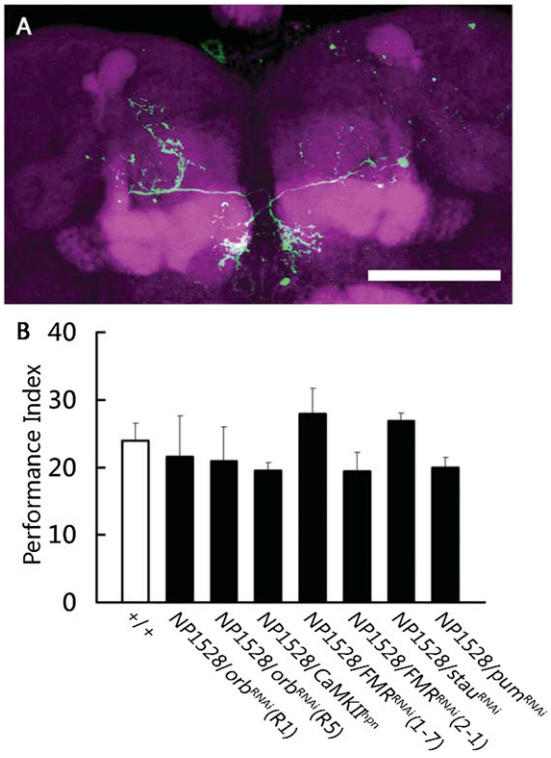

Fig. S10. Normal LTM after RNAi misexpression in the MB-M3 neurons. (*A*) Expression pattern of *NP1528-Gal4* showing specific labeling in the MB extrinsic MB-M3 neurons (green). Brain structures were immunostained with anti-DLG (magenta). (Scale bars, 50 μm.) (*B*) One-day memory was intact after spaced training in flies with constitutive knockdown of ORB, CaMKII, FMR, STAUFEN, or PUMILIO in the MB-M3 neurons. Genotypes: (*A*) *NP1528-Gal4/UAS-mCD8::GFP*. (*B*) (1) +/+, (2) *NP1528-Gal4/+;UAS-orb^{RNAi}(R1)/+*, (3) *NP1528-Gal4/+;UAS-orb^{RNAi}(R5)/+*, (4) *NP1528-Gal4/+;UAS-CaMKII^{hpn}/+*, (5) *NP1528-Gal4/+;UAS-fmr^{RNAi}(1--7)/+*, 6) *NP1528-Gal4/+;UAS-Gal80^{ts}/UAS-fmr^{RNAi}(2–1)*, (7) *NP1528-Gal4/UAS-stau^{RNAi}*, and (8) *NP1528-Gal4/UAS-pum^{RNAi}*.